Hindawi Publishing Corporation
Journal of Fuels
Volume 2015, Article ID 674705, 14 pages
http://dx.doi.org/10.1155/2015/674705

Research Article

DoE Method for Operating Parameter Optimization of a Dual-Fuel BioEthanol/Diesel Light Duty Engine

Gabriele Di Blasio, Mauro Viscardi, and Carlo Beatrice

Internal Combustion Engine Institute, National Research Council, Marconi Street 4, 80125 Naples, Italy

Correspondence should be addressed to Gabriele Di Blasio; g.diblasio@im.cnr.it

Received 30 August 2014; Revised 9 December 2014; Accepted 12 December 2014

Academic Editor: Mingfa Yao

In recent years, alcoholic fuels have been considered as an alternative transportation biofuel even in compression ignition engines either as blended in diesel or as premixed fuel in the case of dual-fuel configuration. Within this framework, the authors investigated the possibility to improve the combustion efficiency when ethanol is used in a dual-fuel light duty diesel engine. In particular, the study was focused on reducing the HC and CO emissions at low load conditions, acting on the most influential engine calibration parameters. Since this kind of investigation would require a significant number of runs, the statistical design of experiment methodology was adopted to reduce significantly its number. As required by the DoE approach, a set of factors (injection parameters, etc.) were selected. For each of them, two levels "high" and "low" were defined in a range of reasonable values. Combining the levels of all the factors, it was possible to evaluate the effects and the weight of each factor and of their combination on the outputs. The results identified the rail pressure, the pilot, and post-injection as the most influential emission parameters. Significant reductions of unburnt were found acting on those parameters without substantial penalties on the global engine performances.

1. Introduction

Future stringent legislations on environmental pollutants and carbon dioxide emissions from diesel engines, together with the need to reduce the fossil fuel dependency, are driving the research towards alternative combustion modes and nonconventional fuel sources.

The recent years have seen an important increment in the use of biofuels as alternative fuels in the transportation sector. In this field, alcoholic biofuels like bioethanol (BE) are receiving considerable attention as valid alternative to conventional fuels in internal combustion engines.

The interest on bioethanol originates from the reasons that it is renewable. It can be produced via alcoholic fermentation of sugar from a different kind of vegetable biomass (first generation bioethanol). Recently, the second generation BE, which utilizes lignocellulosic biomass derived from forest residues, wood wastes, solid wastes, and so forth, has received increased interest because of the abundant low-cost feedstock and because it does not compete with food crops [1]. BE is biodegradable and offers the benefit of reducing the greenhouse gases (GHG). Moreover, BE contributes significantly to particulate emissions reduction because of its intramolecular oxygen content [2]. Due to the low cetane number (CN), BE represents also an important enabler for RCCI (reactivity controller compression ignition) combustion mode [1, 3–6].

On the other hand, literature studies results show that in general bioethanol determines an increase of HC and CO emissions when used in compression ignition engines either in dual fuel configuration or in blend with diesel [4, 7–9].

When alcohol fuels are mixed in blend with diesel fuel, to stabilize the blend (avoiding fuel separation) additives or biodiesel are required to be added. For this reason, the amount of blended alcohol is limited to low percentages [8]. Instead, the alcohol fumigation (premixing in the manifold) has the advantage of providing a variable part of the total fuel adaptable to the operating condition and without adding any additives. However, this method requires limited but more modification of the powertrain configuration (e.g., low

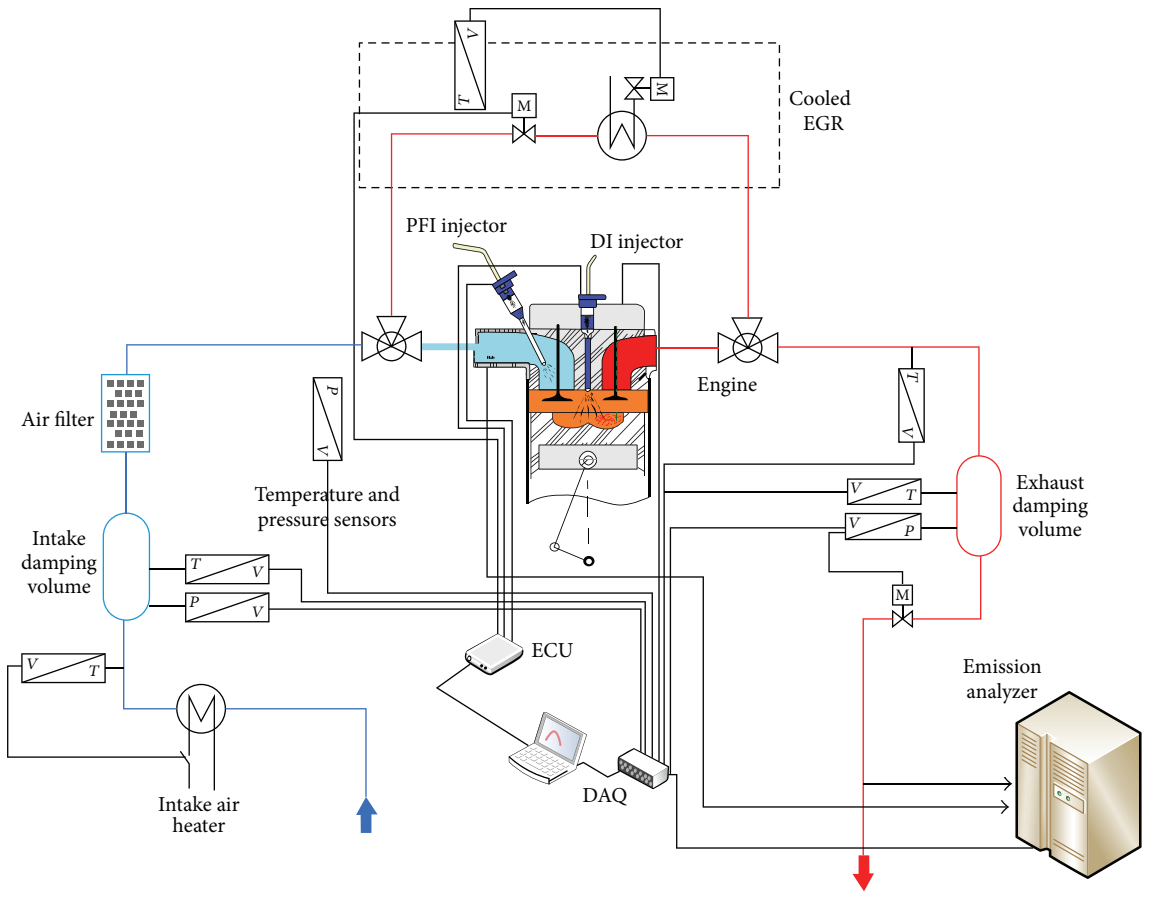

Figure 1: Research engine experimental layout.

pressure fuel injector, separate fuel tank, lines, etc.) compared to the blended case [7].

Aiming at the dual fuel (DF) configuration with port injected BE and direct injected diesel, the research effort was focused on the optimal use of bioethanol on engine performance and emissions using a Euro 5 single cylinder research diesel engine. To this goal, the effect of the engine parameters calibration was evaluated to better exploit the BE characteristics focusing on which are the main affecting parameters on the combustion process evolution in a DF diesel engine employing BE as premixed fuel.

2. Materials and Methods

2.1. Experimental Set Up and Fuels. The experimental activities were conducted on a prototype single cylinder research engine which has a modern combustion system design (manifolds, head, piston, etc.) derived from a Euro5 compliant four cylinders engine which represents the state of the art of light duty (LD) diesel engine technology. The OEM cylinder head has been modified to work in DF mode placing a port fuel injector in the not-swirling runner just upstream the intake valve. Auxiliary systems for boost, cooling, lubrication, and so forth are not directly coupled with the engine in order to allow for a maximum flexibility to control their parameters without influencing the load conditions. The engine layout is laid out in Figure 1, while in Table 1 the main engine characteristics are listed.

A Kistler piezo-quartz transducer fitted inside the combustion chamber was adopted to acquire the pressure traces. The apparent heat release (HR) and rate of heat release (RoHR) were elaborated in real time by the AVL INDIMICRO indicating system. The fuels consumptions were measured by means of two mass flow meters AVL 733. The filter smoke number (FSN) was measured by an AVL 415S smoke meter and cross checked with the AVL Microsoot Sensor when the smoke values where at the limit of the sensitivity of the smoke meter. The gaseous emissions were detected by means of ABB, Ecophysics, and Emerson devices for UHC, NO_x, and CO, CO_2, O_2, respectively.

For the HC measurement the FID technology represents the standard method for the automotive emissions regulation; anyway some recent studies on spark ignition engines have shown that this method has a low sensitivity to oxygenated compounds typically associated with the use of alcohol fuels [10]. Such studies reveal also that, within moderate percentage of alcohol fraction (e.g., ≤20%), the reduction of the FID response factor is below 5%. Therefore, even if in the present work (referred to a diesel engine) the HC values are slightly underestimated for the ethanol blend, the authors

Table 1: Engine characteristics.

Displaced volume	477 cc
Stroke	90 mm
Bore	82 mm
Compression ratio	16.5 : 1
Number of valves	4
Diesel injection system	Common rail
Diesel injector	Centered 7 holes microsac
PFI injector	12 holes

Table 2: Fuel properties.

Feature	Method	Commercial diesel	Bioethanol
Density @ 15°C [kg/m^3]	EN ISO12185	845	790
Cetane number	EN ISO5165	53	8–10
Low heating value [MJ/kg]	ASTMD3338	42.6	27.2
Heat of vaporization [kJ/kg]	—	265	840
Distillation [°C]	EN ISO3405		
	IBP	159	78
	10 [%, vol.]	194	—
	50 [%, vol.]	268	—
	90 [%, vol.]	333	—
	95 [%, vol.]	350	—
	FBP	361	78
Carbon [mol%]	5991	~85.5	52.2
Hydrogen [mol%]	5991	~13.5	13.1
Oxygen [mol%]	5991	~1	34.7

consider the comparative analysis reported in the following not compromised by the raw FID data.

The main characteristics of the fuels used for the blends are listed in Table 2. The commercial diesel is constituted by 93% of mineral diesel and 7% of biodiesel and therefore the commercial diesel is denoted in the paper as "B7." The pure bioethanol characteristics used for the blends are reported in Table 2.

2.2. Testing Methodology. Previous authors activities and some literature studies have shown that the main disadvantage in using BE in DF configuration is the significant increases of unburned hydrocarbons (HC) and carbon monoxide (CO) especially at low load operating conditions [7, 9]. For this reason, the authors have chosen to investigate at low load conditions, in particular at 1500 rpm and 2 bar of BMEP (denoted as 15 × 2), on the most influential parameters in terms of emission reduction.

The first part of the experimental activity was devoted to characterize the engine performance and emissions employing a reference Euro5 parameter calibration and fuelling the engine with B7 fuel. Subsequently, in DF operating conditions, at constant load and engine parameter calibration, premixed BE was injected substituting part of the total quantity of injected B7. For this activity, the mass percentage of premixed BE was fixed at 16% representing the value at which the increment of the unburnt was limited to an acceptable range [7]. Higher levels of BE have been used by the authors in previous studies [7, 9] showing a very sharp increase in CO and HC emissions. Since the aim of the present work is not to evaluate the limit of BE substitution but to assess the most influential engine parameters on the emissions and performances, the authors have chosen a premixing ratio of 16% denoting it as BE16. Moreover, BE has been injected during the intake valve opening period at 360 CAD bTDC.

Table 3: Engine parameters chosen as factors.

Parameter	Factor abbreviation
Rail pressure	P_{rail}
Air mass flow	Q_{air}
Pilot injection quantity	Qpilot
Dwell time pilot-main	DTpilot
Energizing time of post injection	ETpost
Dwell time main-post	DTpost
Swirl	Swirl

The second part of experimental activity was focused on the optimization in the use of the port injected BE in DF configuration, identifying, also, the effect and the corresponding weight of the main engine parameters. To achieve this goal, the statistic methodology, design of experiment (DoE) was adopted.

DoE enables determining simultaneously the *single* and the *interactive* (or *combined*) effects of several parameters, called "*factors,*" which affect the outputs in any design, varying the multiple levels of each factor. Moreover, the experimental design allows identifying the best (or optimum) combination of factor levels, able to achieve the predefined target. More details on DoE can be found in literature [11, 12].

This statistical approach was applied in the present work with the aim to reduce the HC and CO emissions without penalizing the global performances of the engine. On the experience basis seven factors were chosen and shown in Table 3, among the several engine calibration parameters that more likely affect the engine performances and emissions.

As mentioned in Table 3, for each parameter (factor) two levels have been defined: "low" and "high" denoted by the signs minus ("−") and plus ("+"), respectively. Preliminary tests were carried out to identify the low and the high level within reasonable operating limits. Moreover, the low and high level values, of the seven parameters, have been assigned to obtain approximately symmetrical values compared to the reference engine calibration (Table 5). The outputs of these

variations are compared on a graph named *Pareto Anova*, through which it is possible to identify the influence of each factor.

To assess the complete effect of the factors, it should be necessary evaluate all level combinations of the tests by a "full factorial design" (levels^factors = 2^7 = 128). In order to reduce further the number of tests, a "fractional factorial design" has been adopted instead of the full factorial design [11]. This has permitted the authors to halve the number of tests as a consequence of making the "swirl" factor depending on the others. Thus, the final test campaign has been reduced to 2^(7 − 1) = 64 test points.

In this preliminary study, even if influential, EGR was not employed and considered because of the difficulty to keep it precisely constant during the variation of the other parameters. Any variation could foul up the engine outputs since EGR test to test variability could be of the same order of the parameters effects on the output results. Moreover, the tests were performed at fixed combustion barycentre (MBF50 = 7.5 CAD) by varying the start of the main injection (SOI) when necessary. For all engine parameters combination, practical constraints such as maximum values on pressure rise rate ($dP/d\theta$ = 80 bar/ms) and coefficient of variation of IMEP (COV_{IMEP} = 3%) were considered.

The tests were carried out at fixed indicated mean effective pressure (IMEP = 3,3 bar) corresponding to 2 bar of BMEP, acting only on the B7 and/or BE fuel quantities when a deviation from the reference value (due to the factors change) occurred.

The main operating point characteristics object of investigation are listed in Table 4. The factors and the relative levels are shown in Table 5.

To better clarify the authors approach, a brief and explanatory example is described.

The reader images of studying an object "Z" through three (A-B-C) properties (factors) that characterize his behavior. Each property can assume 2 values (levels): high (+1) and low (−1).

In these conditions, to understand the influence of the factors on the behaviour of the object Z using a full factorial design there would be a test campaign planned in 2^3 = 8 tests (Table 6). Instead of using a fractional factorial design, there would be a test campaign planned in 2^(3 − 1) = 4 tests (Table 7).

In the second case, it has been possible to reduce the number of tests making the level of factor C dependent on factors A and B. Indeed his value of each test is obtained from the multiplication of A and B of the same row. For this reason the level of C is obtainable applying the easy rule of signs.

3. Results and Discussion

In this paragraph, the tests results are presented. The analysis and discussion are divided into three parts. Firstly, a comparison of the engine performance and emission outputs between reference B7 and the BE16 is presented. The second part has the aim to analyse the effects of the factors on the performances and emissions with the aim of finding the optimal DF engine parameters calibration (by means of DoE method). At the end a comparison of the engine performances adopting the base and the optimized engine calibration is shown.

Table 4: Test point.

Test point	RPM	IMEP [bar]	BMEP* [bar]	EGR [%]	MBF50 [CAD ATDC]
1500x2	1500	3.3	2	0	7.5

BMEP* of the real four-cylinder engine of equal unit displacement.

Table 5: Factors and levels.

Factor	Level		
	−1	map	1
P_{rail} [bar]	400	600	800
Q_{air} [L/min]	250	310	325
Q_{pil} [mm^3/stroke]	0.60	1.00	1.50
DTpil [μs]	800	1111	1400
ETpost [μs]	150	—	250
DTpost [μs]	800	—	1200
Swirl [%]	20	65	90

Table 6

Full factorial design			
Factor	A	B	C
Test 1	−1	−1	−1
Test 2	−1	−1	1
Test 3	−1	1	−1
Test 4	−1	1	1
Test 5	1	−1	−1
Test 6	1	−1	1
Test 7	1	1	−1
Test 8	1	1	1

Table 7

Fractional factorial design			
Factor	A	B	C
Test 1	−1	−1	**1**
Test 2	−1	1	**−1**
Test 3	1	−1	**−1**
Test 4	1	1	**1**

3.1. Emission and Performance Analysis. In Figure 2 the comparison of the regulated emissions emitted by the engine in conventional and DF configuration is shown. In DF mode, there is a slight NO_x and soot reduction, but at the same time with a strong HC and CO increase compared to reference B7 case.

The reduction on smoke is mainly due to the presence of intramolecular oxygen in BE [5, 13–15]. In fact, the presence of bonded oxygen enhances the soot oxidation rate and reduces the formation of soot nuclei in locally

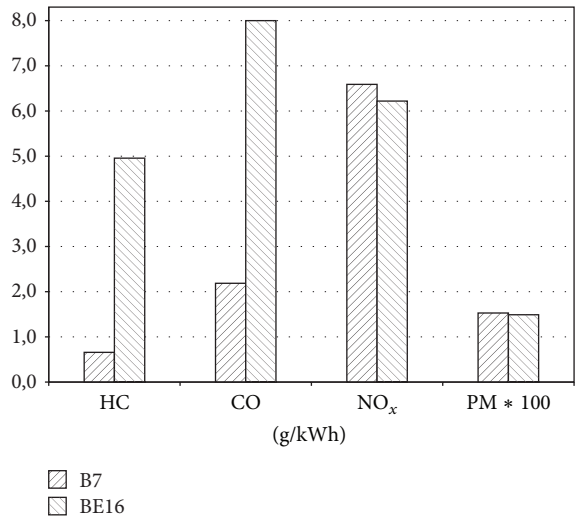

Figure 2: Emissions comparison between B7 and BE16.

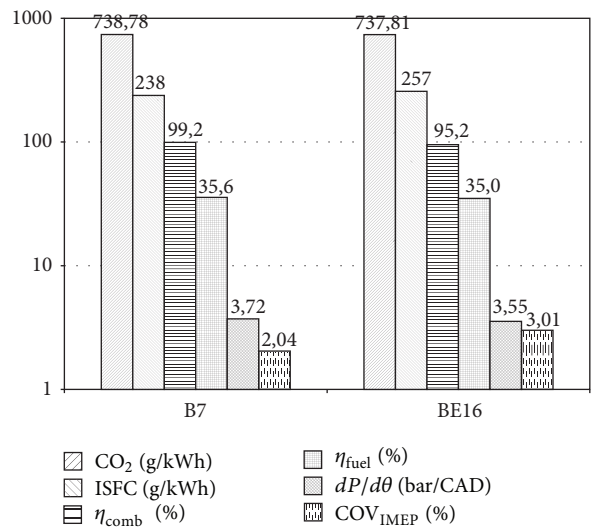

Figure 3: Comparison between B7 and BE16 in terms of specific consumption, efficiencies, combustion noise, and stability.

rich zones [13, 15]. Moreover, the reduction of aromatics content, the lower C/H mass ratio (see Table 2), and the lower surface tension and boiling point (that promote the spray characteristics [15] improving the air/fuel mixing) also contribute to the smoke reduction.

The DF NO_x emissions decrease is due to the lowering of the in-cylinder temperature peak as the BE increase (Figure 4) and a consequence of the higher latent heat of vaporization of BE [16]. Indeed, the cooling effect of BE seems to be dominant with respect to the higher oxygen content that could counteract the NO_x emissions reduction.

Another expected result is the sharp increase of unburned gas emissions and carbon monoxide of BE16, shown in Figure 2. First of all, this result is consistent with the reduction of the combustion efficiency (indicated as *eta comb*) shown in Figure 3. Among the causes of HC and CO increment, an important role is played by the CN reduction that contribute to the lower pilot combustion efficiency and then contributing to the increment of unburned emissions. Moreover, as observed by other authors [13, 17], the high premixing level of bioethanol together with the higher heat of vaporization causes local cooling and even flame quenching when the temperature chamber is relatively low. These effects also contribute to lower the combustion stability as stated by the increase in COV. All these characteristics and phenomenon have an important role both on HC emissions increment and on CO conversion in CO_2.

In Figure 3 the indicated specific fuel consumption (ISFC) and the fuel conversion efficiency (η_{fuel}) are reported. In particular, the fuel efficiency (η_{fuel} or *eta fuel*) was calculated following the equations reported in the appendix [18]. A reduction of the overall efficiency is observable. This result is consistent with the ISFC increment when BE is employed in DF mode. The lower LHV_{mix} counteracted only partially the reduction of the fuel efficiency and this is explainable by a general decrease of the combustion efficiency.

In Figure 4 the in-cylinder pressure and heat release (HR) evolution versus crank angle degree (CAD) are also reported. The pressure traces show lower compression and combustion peaks in DF case compared to the reference blend (Figure 4(a)). The lower compression peak is attributable to the BE cooling effect that consequently affect the combustion peak too.

The heat release (HR) and the rate of heat release (HRR) traces (Figure 4(b)) evidence a delay of the pilot RoHR in the case of BE16. This is attributable to the dilution effect (lower charge reactivity) of the premixed ethanol. The lower charge reactivity slows down the combustion rate and as a consequence, there is a slightly more diffusive pattern characterized by lower flame temperature and higher unburnt. The combination of these effects with those linked to the higher latent heat of vaporization of the ethanol justifies the NO_x emissions reduction (Figure 2) as well as the lower thermal efficiency of the DF working at low load conditions (Figure 3).

3.2. Effect of Engine Parameter Calibration. In this section the effects on the HC and CO emission of the chosen engine calibration parameters (factors) evaluated implementing the DoE statistical method are presented. In the following, for brevity, only the most significant results are reported.

Even if this activity was mainly focused on the HC and CO reduction, for a more comprehensive study the factor effects on NO_x, soot, CO_2, ISFC, efficiencies, COV_{IMEP}, and pressure rise rate ($dP/d\theta$) were also evaluated. This permits suggesting alternative DF engine calibration able to lower the HC and CO emissions without significant issues on the engine working functionality.

In Figures 5 and 6, two types of diagrams are presented. The bar graph, representative of the Pareto Anova, shows the individual effect (of each factor) and the interactive effect (combination of two factors) on the output results. The second graph shows the individual and interactive absolute

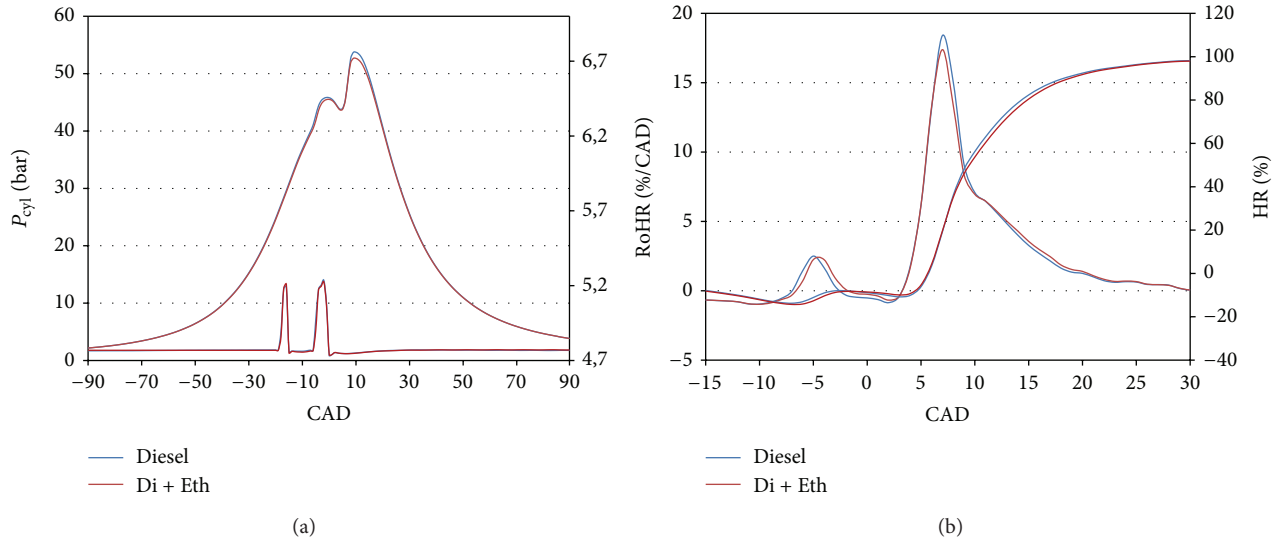

Figure 4: Cylinder pressure and energizing current (a); RoHR and HR (b) for B7 and BE16 at 1500 rpm and 2 bar of BMEP.

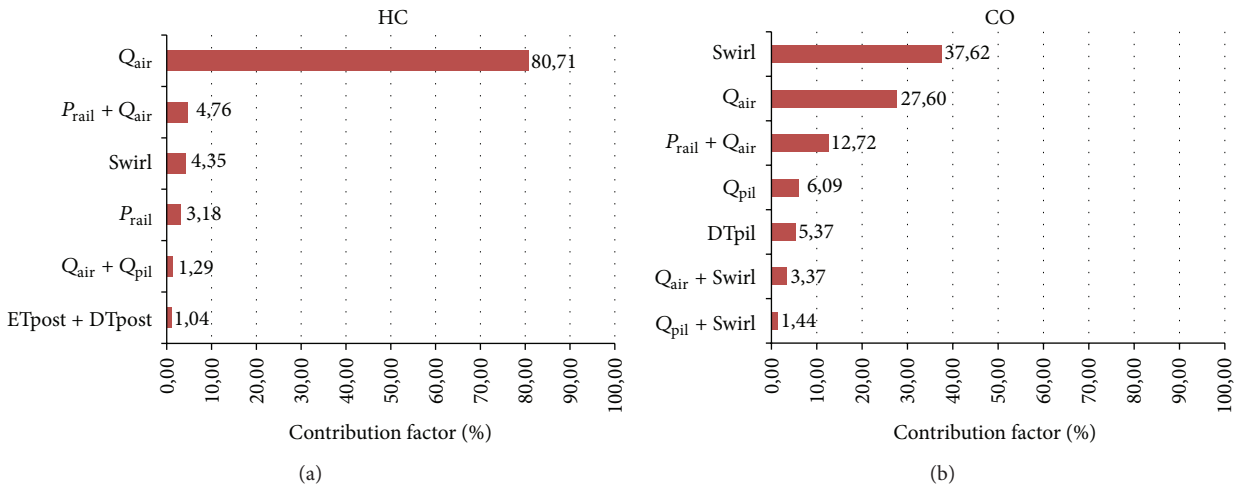

Figure 5: Pareto Anova HC (a) and CO (b).

variation of each and two parameters. For brevity, only the most influential factors on the engine outputs are presented.

The effects of all parameters influencing the HC and CO are shown in Figure 5. For what concerns the HC, the influence of the Q_{air} factor variation (about 80%) is very prominent. The other effects are of minor importance (e.g., P_{rail} + Q_{air} = 4,76%, *Swirl* = 4,35%, etc.). In Figure 6 the absolute HC reduction is shown when the air mass flow rate is at the lower level. In fact, a lower air/ethanol ratio is more favourable in relation to the flammability range, allowing an improvement of the combustion rate and then of the efficiency (see Figures 9 and 10). Furthermore, a lower air/fuel ratio increases the charge temperature reducing the flame quenching probability.

The increase of *Swirl* and P_{rail} has a smaller but not negligible effect on HC reduction. The combined factors "P_{rail} + Q_{air}" effect is shown in Figure 6. When the P_{rail} rises from the lower to the upper level, at lower air flow rate (red segment) it has negligible effect on HC. However, for higher air flow rates (blue segment), the oxygen content within the air/fuel mixture will definitely be greater, so the increase of the injection pressure allows to reduce the size of the fuel droplets and increase their kinetic energy obtaining a better mixing of the charge and a more complete combustion. Both of these aspects justify a reduction of HC emission. The best result in terms of HC reduction is when the Q_{air} is low and P_{rail} is high. The *Swirl* influence is related to the need of a stronger air motion at lower engine speeds to obtain a better air-fuel mixing. As the swirl motion increases, more BE is involved during the combustion process with a consequent HC reduction (Figure 6).

Similar considerations are also valid for the CO emission trend (Figures 5 and 6). The most affecting factors are *Swirl* (about 37%), Q_{air} (27,6%) and the interaction of P_{rail} + Q_{air} (12,7%). Furthermore, an increase and advance of the pilot injection (Q_{pil} and DTpil, resp.), together with

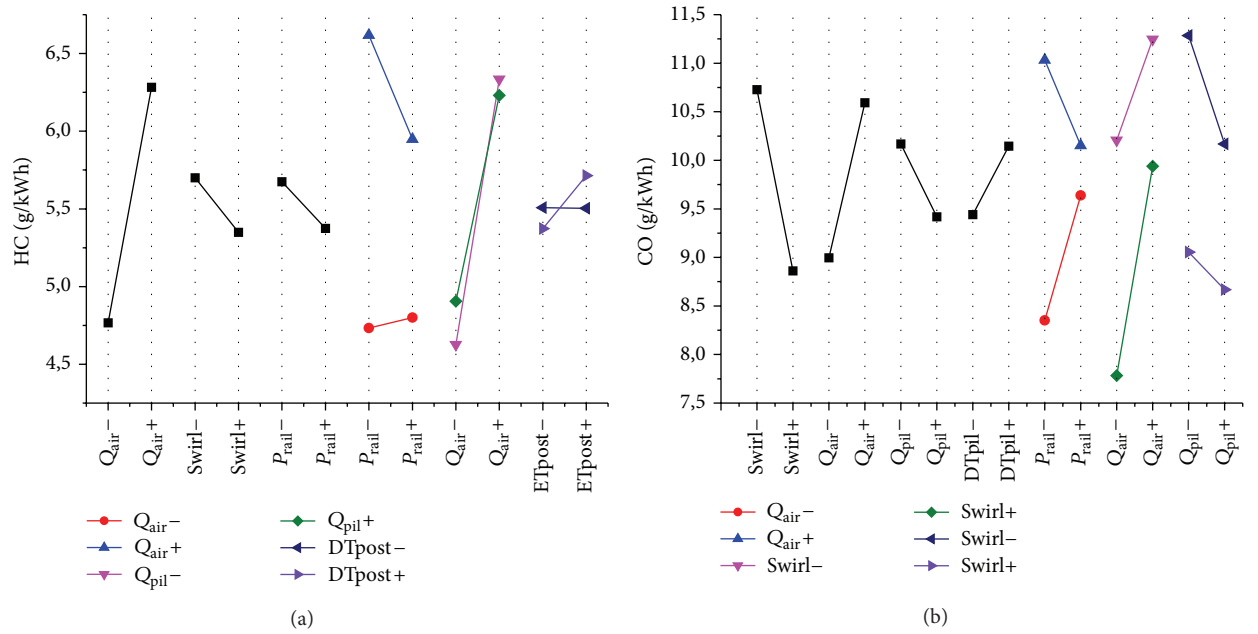

Figure 6: Individual and interactive absolute variation of each or/and two parameters of HC (a) and CO (b).

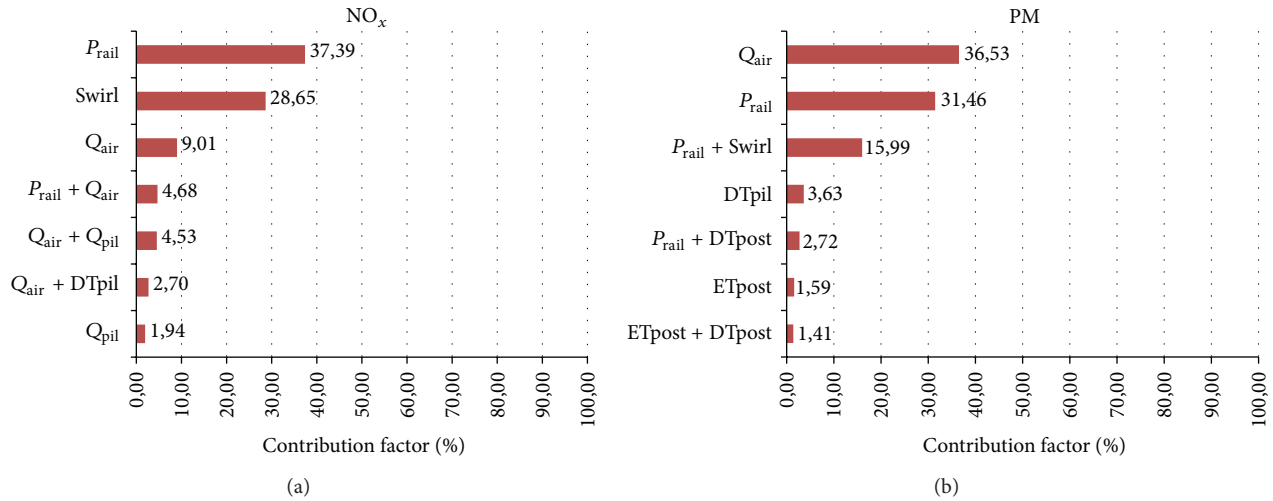

Figure 7: Pareto Anova NO_x (a) and PM (b).

the abovementioned factors, produce a CO reduction. This is attributable to a general increase of the in-cylinder temperatures. The increase of the pilot fuel and the advance of its injection counteract the ethanol cooling effect that causes a higher ignition delay (ID) and flame quenching.

As for the HC trend, for lower Q_{air} (red segment), as the P_{rail} increases the CO rises (Figure 6). The trend could be explained by a higher fuel jet penetration when the charge density in the combustion chamber is higher. Indeed, if the density is too low, the tip of the jet could have an impact on the cylinder liner amplifying the quenching phenomenon and thus lowering the temperatures and then worsening the CO oxidation to CO_2. There is a reverse trend when the Q_{air} is at higher levels (blue segment).

Concerning the NO_x emissions, lower rail pressures means also lower NO_x emissions (Figures 7 and 8). A lower atomization worsens the air-fuel mixing and then the combustion temperatures. Also lower swirl levels reduce the HC oxidation rates and consequently the NO_x emissions (as shown in Figure 8). Lower Q_{air} reduces the in-cylinder pressure and thus the temperatures during the compression stroke.

Conversely, the PM trend should be opposed to the NO_x one (trade-off). Indeed, both larger fuel droplets (lower P_{rail}) and less turbulence in the combustion chamber cause a stronger PM production as shown in Figures 7 and 8. The PM reduction for lower Q_{air} shown in Figure 8 is not common, but since the equivalence ratio in this point is very low (low load

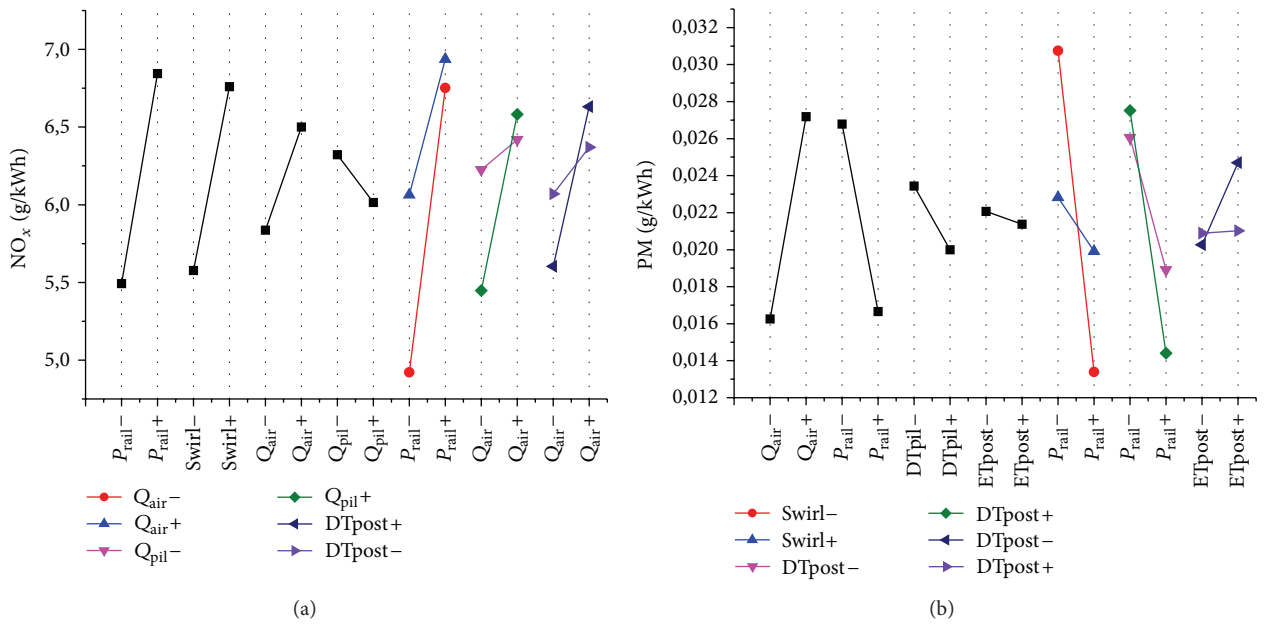

FIGURE 8: Individual and interactive absolute variation of each or/and two parameters of NO_x (a) and PM (b).

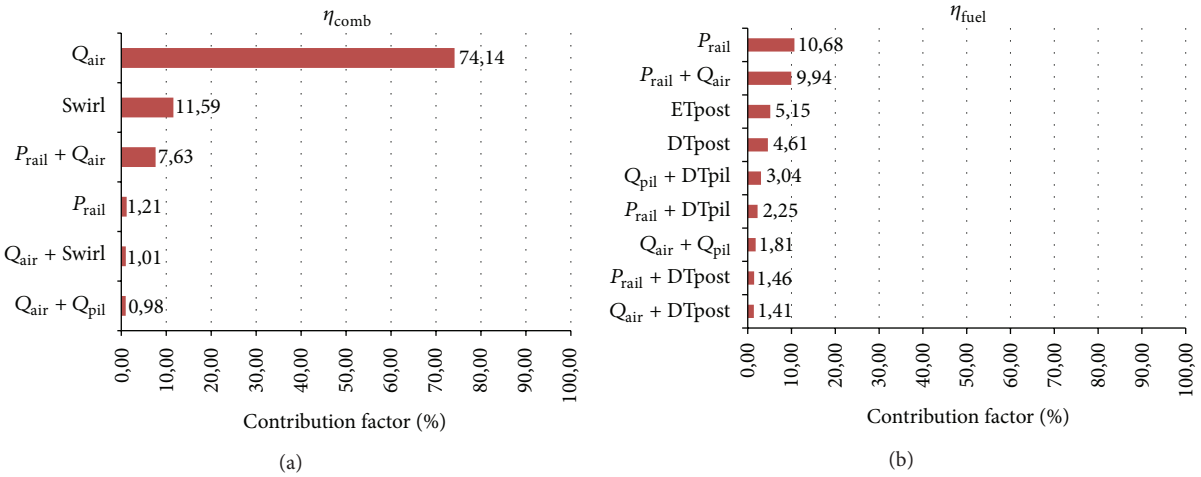

FIGURE 9: Pareto Anova combustion efficiency (a) and fuel efficiency (b).

operating conditions), higher ratio could affect positively the soot oxidation ratio. However, the PM in this operating point is at very low levels and the increase is not significant.

The results in terms of CO_2, ISFC, COV_{IMPEP}, and pressure rise rate ($dP/d\theta$) are reported in the Appendix (Figures 14, 15, 16, and 17). The discussion is here omitted for brevity.

3.3. Optimized Calibration Analysis. In this paragraph the comparison among the engine performances of the test points in DF operating mode adopting the reference calibration (BE16), the optimized parameters calibration (test number) and the reference diesel calibration in conventional (not DF) configuration (B7) is presented.

Among the performed tests (32 runs), four tests were chosen which ensured the best compromise in terms of emissions, efficiency, combustion stability, and pressure rise rate (Figure 11). They are reported in Table 8.

Concerning the combustion efficiencies (η_{comb}), the one using B7 is always higher compared to those related to the DF configuration with the optimal calibration explored by DoE method (Figure 12). Indeed, in DF operating conditions, the higher unburnt (mainly constituted by ethanol are directly linked to the combustion efficiency reduction (see Figure 11) [7, 9]. On the other hand, the lower η_{comb} is partially counteracted by a slightly higher thermodynamic efficiency (faster combustion rate around the TDC). Thus, the DF η_{fuel} is only a little lower and therefore almost constant (Table 10).

On the other hand a significant $dP/d\theta$ and COV_{IMEP} reduction was observed together with a little improvement of the CO_2 reduction. Since the global efficiency is nearly

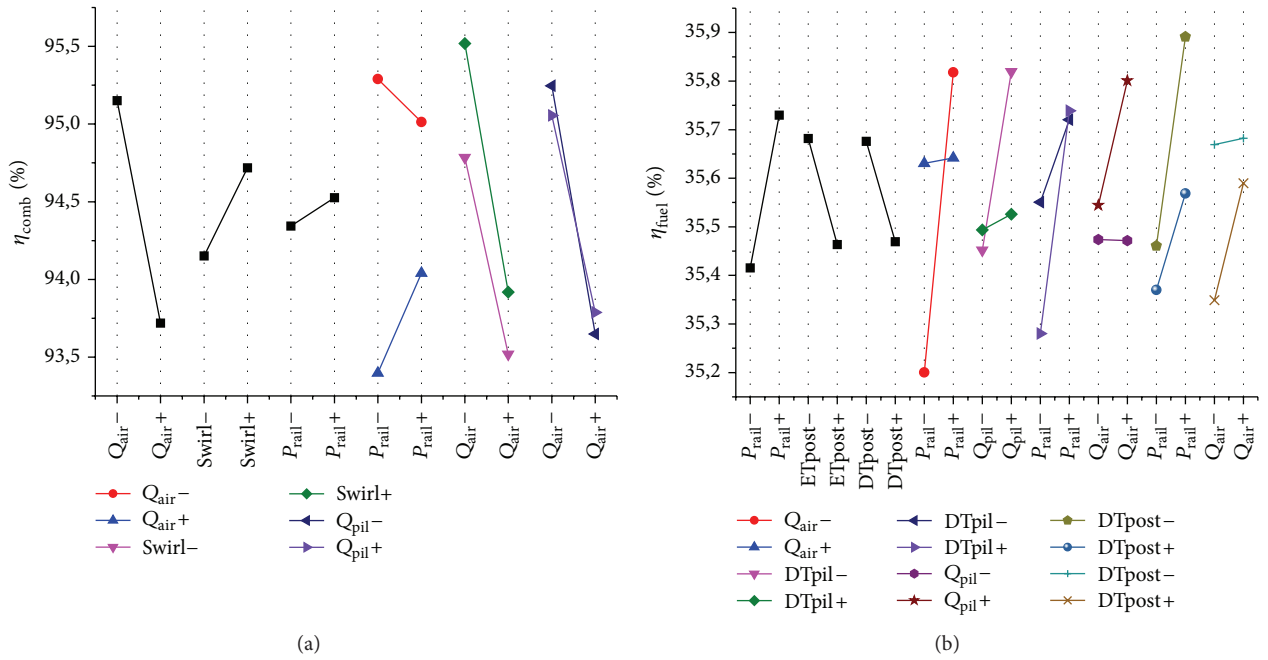

Figure 10: Individual and interactive absolute variation of each or/and two parameters of combustion (a) and fuel efficiency (b).

Table 8: Factors, levels, and engine parameter calibration of tests 4, 6, 12, and 13.

	Factors and levels						
	P_{rail}	Q_{air}	Q_{pil}	DTpil	ETpost	DTpost	Swirl
Test 4	−1	−1	−1	−1	1	1	1
Test 6	−1	−1	−1	1	−1	1	1
Test 12	−1	−1	1	−1	1	1	−1
Test 13	−1	−1	1	1	−1	−1	1
	[bar]	[L/min]	[mg/stroke]	[μs]	[μs]	[μs]	[%]
Test 4	400	250	0,60	800	250	1200	90
Test 6	400	250	0,60	1400	150	1200	90
Test 12	400	250	1,50	800	250	1200	20
Test 13	400	250	1,50	1400	150	800	90

constant, the CO_2 enhancement is mainly related to the more favourable C/H ratio of bioethanol compared to commercial diesel.

As reported in Figure 12, the test which more achieves the predefined goal (lower unburnt without scarifying the global performances) is test 13 (Figures 11 and 12). The calibration parameters setting of this test point is reported in Table 9.

Compared to the map calibration, the optimized calibration has a lower rail pressure, a reduced air flow rate, a higher swirl rate, a higher pilot fuel quantity, and an advanced pilot phasing. Moreover, the optimized calibration was achieved by adding a little postinjection very close to the main injection. The pressure cycles and the energizing current of the optimal test point are shown in Figure 13(a) where the reference diesel traces (B7) and the DF traces related to the map calibration (BE16) are also reported.

The pressure traces clearly show the lower in-cylinder trapped charge (mainly constituted by air) of the test number 13 in comparison to the map calibration. Indeed, the compression stroke evolves at lower pressures and the pressure peaks are about 8 bars lower.

Table 9: Comparison between the map calibration and the optimized calibration.

	Map calibration	Optimized calibration
P_{rail} [bar]	600	400
Q_{air} [L/min]	310	250
Q_{pil} [mm^3/stroke]	1.00	1.50
DTpil [μs]	1111	1400
ETpost [μs]	—	150
DTpost [μs]	—	800
Swirl [%]	65	90

In Figure 13(b), the HR and the RoHR of these operating points are represented. In the case of test 13, the pilot HR

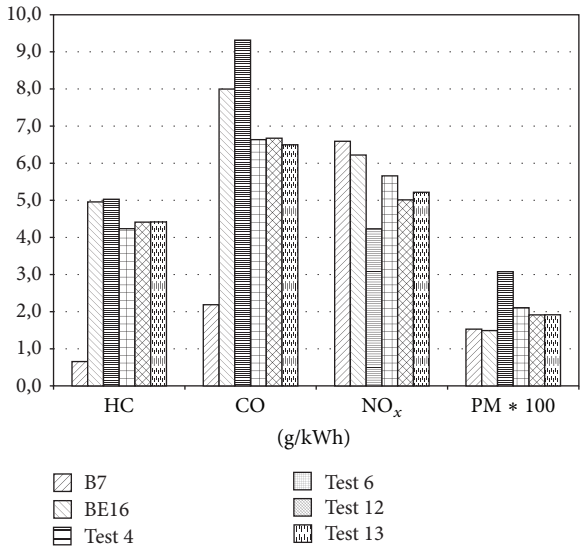

Figure 11: Comparison among B7, BE16, and the optimal tests of the test campaign in terms of emissions.

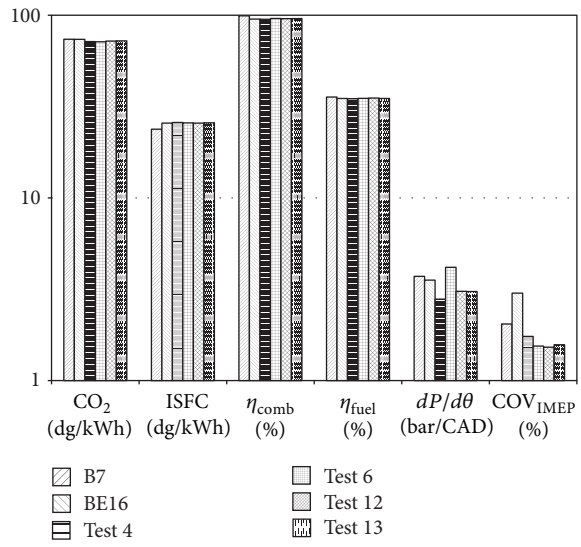

Figure 12: Comparison among B7, BE16, and the optimal tests of the test campaign in terms of efficiencies, combustion stability, and $dP/d\theta$.

is delayed and is closer to the main combustion. As a consequence, the pilot combustion and the first part of the main combustion evolve nearer to the TDC consequently increasing the thermodynamic efficiency. The delay of the pilot HR is due to the lower in-cylinder trapped mass that delays the thermodynamic conditions at which the diesel fuel autoignite.

The comparison among the results of the three test points in terms of emission, efficiencies, ISFC, $dP/d\theta$, and COV_{IMEP} is shown in Table 10. The optimized calibration (test 13) compared to the BE16 base calibration presents a reduction of HC, CO, NO_x, and CO_2 of about 11%, 19%, 17%, and 2%, respectively. On the other hand, the PM increases to about 28,5%, but the absolute PM value is at very low levels. For what concerns the performances, test 13 shows approximately the same results of the BE16 reference calibration. The reduction in terms of $dP/d\theta$ and COV_{IMEP} is about 11% and 50%, respectively. It is worth noting that the combustion "uniformity" (COV_{IMEP}) and the pressure rise rate ($dP/d\theta$) that are critical aspects of the DF combustions improve substantially.

Table 10: Comparison in terms of emissions and performances among the B7, BE16, and the optimal test.

	B7	BE16	DoE15x2_013
HC [g/kWh]	0.7	5	4.4
CO [g/kWh]	2.2	8.0	6.5
NO_x [g/kWh]	6.6	6.2	5.2
PM ∗ 100 [g/kWh]	1.5	1.5	1.9
CO_2 [g/kWh]	739	738	723
ISFC [g/kWh]	238	257	257
η_{comb} [%]	99.2	95.2	95.8
η_{thermo} [%]	35.9	36.8	36.6
η_{fuel} [%]	35.6	35	35
$dp/d\theta$ [bar/CAD]	3.7	3.5	3.1
COVIMEP [%]	2.0	3.0	1.6

4. Conclusions

The present paper focuses on the experimental activity aimed to evaluate the advantages and issues related to an engine parameter optimization when using bioethanol as premixed fuel and commercial diesel as direct injected fuel, on performance and emissions of a Euro5 single cylinder research automotive diesel engine.

The study reveals that, in the tested operating point, the use of bioethanol offers a reduction of NO_x and PM emission compared to the reference blend. The drawbacks concerning the BE use are associated with an increment of unburned emissions mainly linked to the chemical-physical properties of BE. In this regard, the presented study focused on the low engine speed and load conditions since they are the most critical conditions concerning the unburnt.

With the aim to overcome the issues of a strong CO and HC increment, a specific test campaign based on the DoE method was applied to identify the potentiality offered by a proper calibration of the main engine parameters in order to optimize the use of premixed BE.

The study outlines that the most influential engine parameters in terms of HC and CO reduction and the consequent combustion efficiency increase are the air flow rate, the *Swirl*, and the postinjection.

In addition to the above parameters the NO_x, PM, and CO_2 emissions are strongly affected by the rail pressure. Moreover, a particular combination of rail pressure and air flow rate has a strong influence on several of the above monitored outputs.

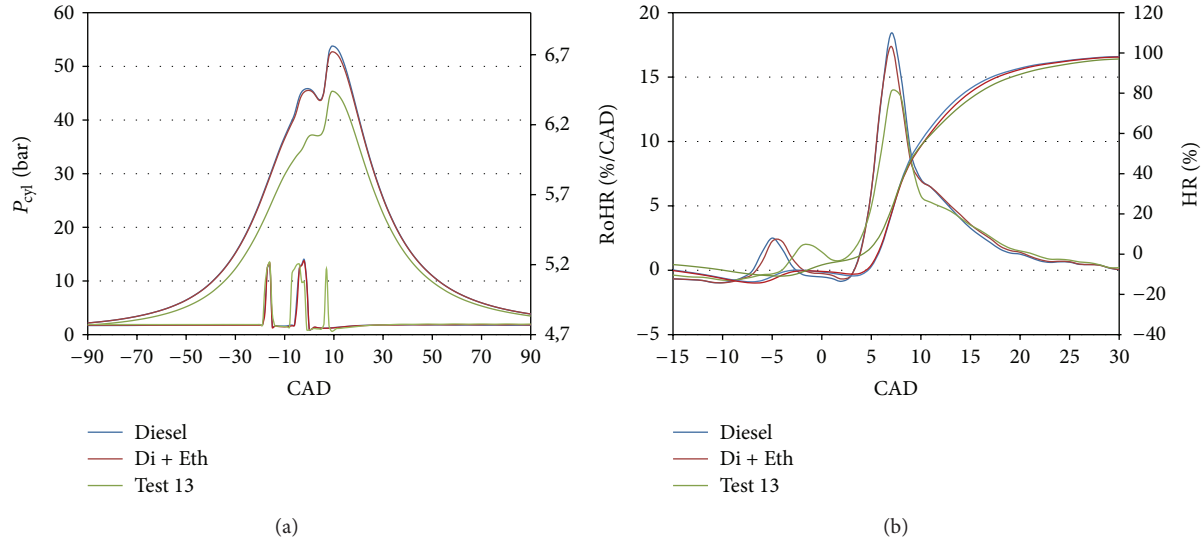

Figure 13: Comparison among B7, BE16, and test 13 of in-cylinder pressure and injection profiles (a) and of HR and RoHR (b).

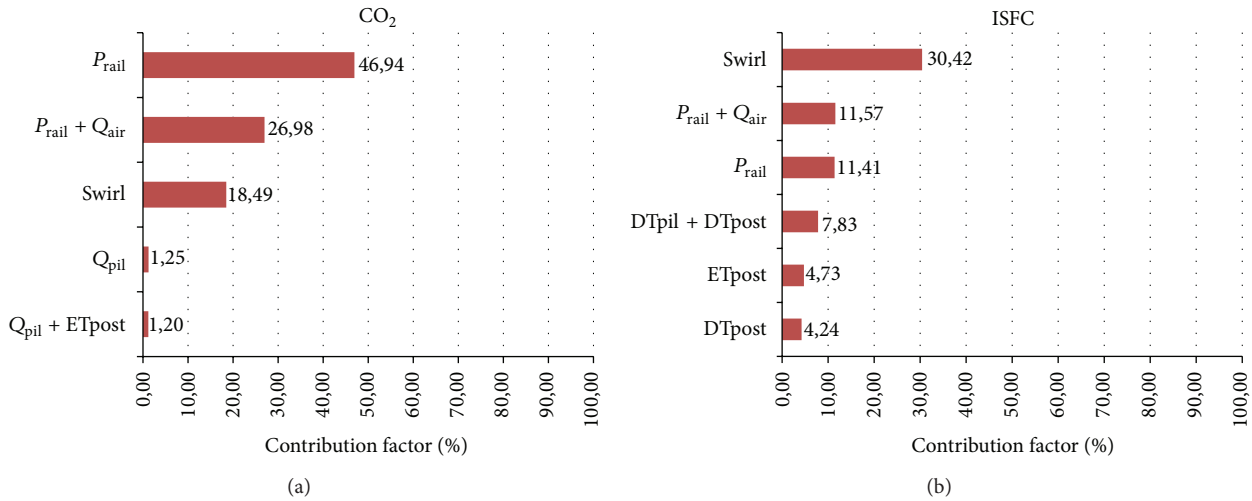

Figure 14: Pareto Anova CO_2 (a) and ISFC (b).

The results demonstrate the possible improvements of bioethanol use. Moreover, the quality of the DoE results suggests the opportunity to integrate this methodology in an automatic engine calibration optimization procedure. In this way, the robustness and the efficiency of the engine calibration can be more easily enhanced. This aspect, in the authors' opinion, cannot be neglected, also considering that, due to the chemical-physical characteristic of alcohol fuels, in some operative conditions so as at low speed and loads it may be the risk of exhaust temperatures below the threshold oxy-catalyst activation.

Future activities will extend the DoE investigation in a wider range of operating area in order to improve the knowledge of the DF combustion process and its most influential engine parameters, permitting a better exploitation of the alternative fuels characteristics in relation to the engine technology.

Appendix

Definition of Premixed Ratio

The premixing ratio on mass basis (r_p) can be quantified according to the following equation:

$$r_p = \frac{m_p}{m_p + m_d} = \frac{m_p}{m_{tot}}, \tag{A.1}$$

where m_p and m_d indicate the mass flow rate of premixed fuel (PFI) and directly injected fuel (DI), respectively.

The r_p is also used for the calculation of the average low heating value (LHV) of the total fuel (DI + PFI):

$$\mathrm{LHV}_{mix} = r_p \cdot \mathrm{LHV}_p + \left(1 - r_p\right) \cdot \mathrm{LHV}_d. \tag{A.2}$$

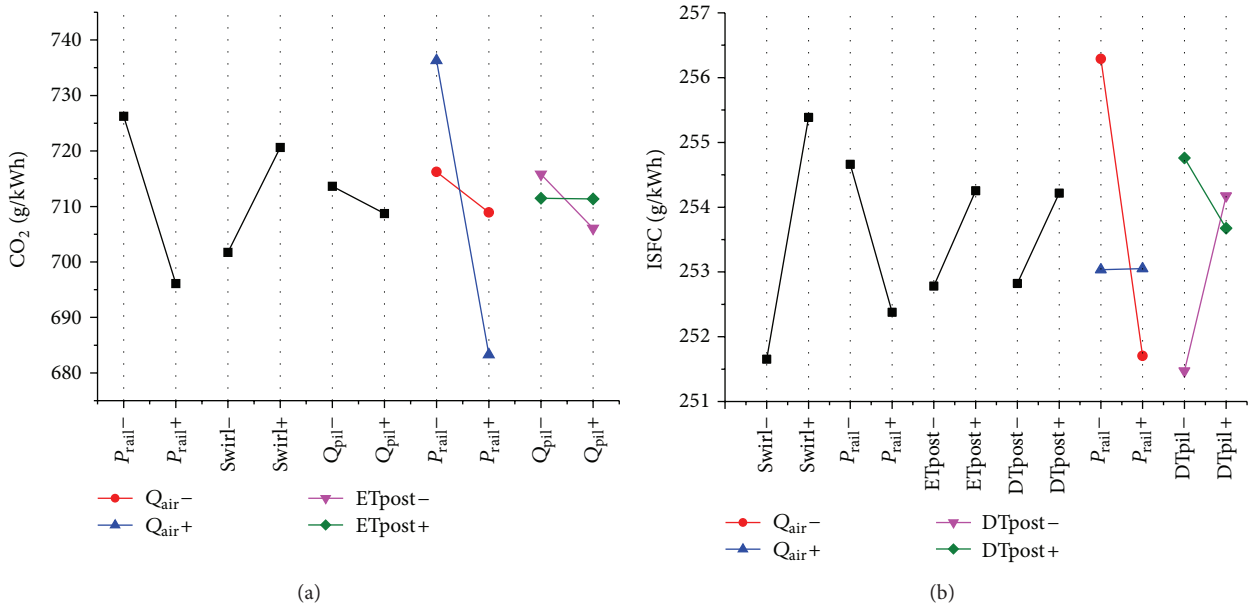

FIGURE 15: Individual and interactive absolute variation of each or/and two parameters of CO_2 (a) and ISFC (b).

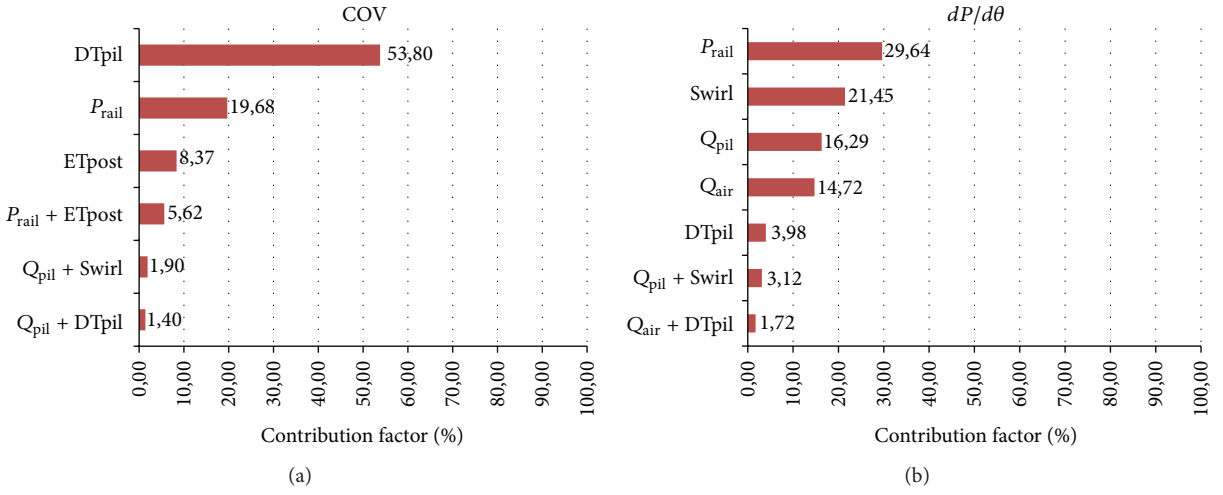

FIGURE 16: Pareto Anova combustion COV_{IMEP} (a) and fuel $dP/d\theta$ (b).

The fuel efficiency is calculated as

$$\eta_{\text{fuel}} = \frac{1}{\text{ISFC} \cdot \text{LHV}_{\text{mix}}} = \eta_{\text{comb}} \cdot \eta_{\text{thermal}}, \quad \text{(A.3)}$$

where the LHV_{mix} represents the mean low heat value of blend in combustion chamber, calculated as

$$\text{LHV}_{\text{mix}} = r_{pm} \cdot \text{LHV}_p + \left(1 - r_{mp}\right) \cdot \text{LHV}_d, \quad \text{(A.4)}$$

while the η_{comb} and η_{thermal} are the combustion and thermal efficiency , respectively:

$$\eta_{\text{comb}} = \frac{Q_i}{m_c \cdot \text{LHV}_{\text{mix}}}$$
$$\eta_{\text{thermal}} = \frac{L_i}{Q_i}. \quad \text{(A.5)}$$

Abbreviations

B7: Fuel blend: 93% volume of diesel and 7% volume of biodiesel
BE16: Direct injection: 84% en masse of B7 premixed injection: 16% en masse of bioethanol
BMEP: Brake mean effective pressure
BSFC: Brake specific fuel consumption
CO: Carbon monoxide
COV: Cycle of variation
DI: Direct injection
DoE: Design of experiment
DTpil: Dwell time from pilot to main injection
DTpost: Dwell time from main to postinjection

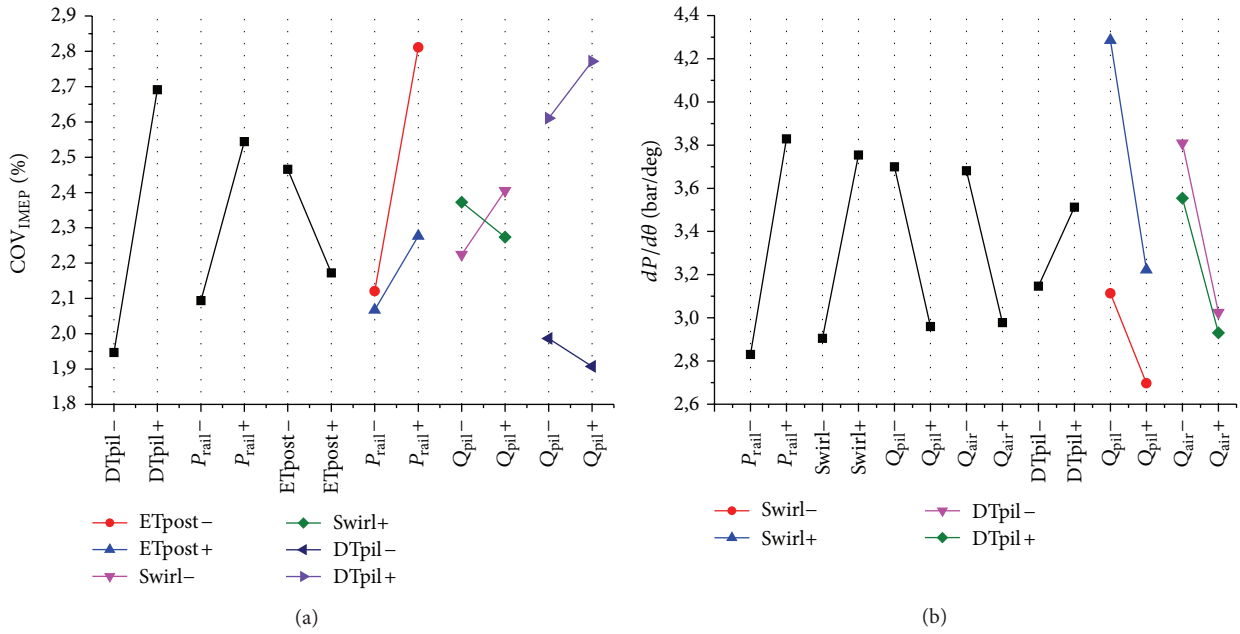

FIGURE 17: Individual and interactive absolute variation of each or/and two parameters of COV_{IMEP} (a) and fuel $dP/d\theta$ (b).

ETpost: Injector's energizing time of postinjection
ECU: Electronic control unit
EGR: Exhaust gas recirculation
FID: Flame ionization detector
FSN: Filter smoke number
HC: Total unburned hydrocarbon
HR: Heat release
GHG: Greenhouse gases
IMEP: Indicated mean effective pressure
ISFC: Indicated specific fuel consumption
LD: Light duty
LHV: Lower heating value
MBF50%: 50 percent of mass burned fraction
NEDC: New European driving cycle
NO_x: Nitrogen oxides emissions
PCCI: Premixed charge compression ignition
PFI: Port fuel injection
PM: Particulate matter
P_{rail}: Rail pressure
Q_{air}: Air flow rate
Q_{pil}: Pilot quantity
RCCI: Reactivity controlled compression ignition
ROHR: Rate of heat release
rpm: Revolution per minute
SOI: Start of main injection
TDC: Top dead center.

Conflict of Interests

The authors declare that there is no conflict of interests regarding the publication of this paper.

Acknowledgments

The authors thank Mr. Alessio Schiavone, Mr. Roberto Maniscalco, and Mr. Augusto Piccolo for their technical support in the engine testing.

References

[1] U. Larsen, T. Johansen, and J. Schramm, "Ethanol as a fuel for road transportation," Main Report EFP06, IEA Implementing Agreement on Advanced Motor Fuels, 2009.

[2] N. P. Komninos and C. D. Rakopoulos, "Numerical investigation into the formation of CO and oxygenated and nonoxygenated hydrocarbon emissions from isooctane- and ethanol-fueled HCCI engines," *Energy and Fuels*, vol. 24, no. 3, pp. 1655–1667, 2010.

[3] R. Dijkstra, G. Di Blasio, M. Boot et al., "Assessment of the effect of low cetane number fuels on a light duty CI engine: preliminary experimental characterization in PCCI operating condition," SAE Technical Paper 2011-24-0053, 2011.

[4] G. Di Blasio, C. Beatrice, R. Dijkstra, and M. Boot, "Low cetane number renewable oxy-fuels for premixed combustion concept application: experimental investigation on a light duty diesel engine," SAE Technical Paper 2012-01-1310, 2012.

[5] B.-Q. He, S.-J. Shuai, J.-X. Wang, and H. He, "The effect of ethanol blended diesel fuels on emissions from a diesel engine," *Atmospheric Environment*, vol. 37, no. 35, pp. 4965–4971, 2003.

[6] V. Fraioli, G. Di Blasio, E. Mancaruso et al., "Experimental and numerical investigations on compression ignition engines using ethanol in dual-fuel configuration," in *Conference on Thermo- and Fluid Dynamic Processes in Direct Injection Engines (THIESEL '12)*, 2012.

[7] G. Di Blasio, C. Beatrice, and S. Molina, "Effect of port injected ethanol on combustion characteristics in a dual-fuel light duty diesel engine," SAE Technical Paper 2013-01-1692, 2013.

[8] P. Napolitano, C. Guido, C. Beatrice, and G. Di Blasio, "Study of the engine parameters calibration to optimize the use of bio-ethanol/RME/diesel blend in a Euro5 light duty diesel engine," SAE Technical Paper 2013-01-1695, 2013.

[9] G. Di Blasio, M. Viscardi, M. Alfè et al., "Analysis of the impact of the dual-fuel ethanol-diesel system on the size, morphology, and chemical characteristics of the soot particles emitted from a LD diesel engine," SAE Technical Paper 2014-01-1613, 2014.

[10] T. Wallner, "Correlation between speciated hydrocarbon emissions and flame ionization detector response for gasoline/alcohol blends," *Journal of Engineering for Gas Turbines and Power*, vol. 133, no. 8, Article ID 082801, 8 pages, 2011.

[11] S. H. Park, *Robust Design and Analysis for Quality Engineering*, Chapman & Hall, London, UK, 1996.

[12] R. Unal and E. B. Dean, "Taguchi approach to design optimization for quality and cost: an overview," in *Proceedings of the 13th Annual Conference of the International Society of Parametric Analysts*, 1991.

[13] M. Lapuerta, O. Armas, and J. M. Herreros, "Emissions from a diesel-bioethanol blend in an automotive diesel engine," *Fuel*, vol. 87, no. 1, pp. 25–31, 2008.

[14] H. Chen, S.-J. Shuai, and J.-X. Wang, "Study on combustion characteristics and PM emission of diesel engines using ester-ethanol-diesel blended fuels," *Proceedings of the Combustion Institute*, vol. 31, pp. 2981–2989, 2007.

[15] L. Zhu, C. S. Cheung, W. G. Zhang, and Z. Huang, "Combustion, performance and emission characteristics of a DI diesel engine fueled with ethanol-biodiesel blends," *Fuel*, vol. 90, no. 5, pp. 1743–1750, 2011.

[16] S. H. Park, I. M. Youn, and C. S. Lee, "Influence of ethanol blends on the combustion performance and exhaust emission characteristics of a four-cylinder diesel engine at various engine loads and injection timings," *Fuel*, vol. 90, no. 2, pp. 748–755, 2011.

[17] M. S. Kumar, A. Kerihuel, J. Bellettre, and M. Tazerout, "Ethanol animal fat emulsions as a diesel engine fuel—part 2: engine test analysis," *Fuel*, vol. 85, no. 17-18, pp. 2646–2652, 2006.

[18] J. B. Heywood, *Internal Combustion Engine Fundamentals*, McGraw-Hill Higher Education, 1989.